IOP Publishing Journal of Physics: Condensed Matter
J. Phys.: Condens. Matter **32** (2020) 145001 (7pp) https://doi.org/10.1088/1361-648X/ab63e5

First-principles study of cohesion strength and stability of titanium–carbon interfaces using vdW interaction

Liang Chen[1,2], Junming Luo[1,2,4], Qian Wang[1,4], Lei Xiong[1,2] and Haoran Gong[3]

[1] School of Materials Science and Engineering, Nanchang Hangkong University, Nanchang, Jiangxi 330063, People's Republic of China
[2] Jiangxi Provincial Engineering Research Center for Surface Technology of Aeronautical Materials, Nanchang Hangkong University, Jiangxi 330063, People's Republic of China
[3] State Key Laboratory of Powder Metallurgy, Central South University, Changsha, Hunan 410083, People's Republic of China

E-mail: qwqianw@163.com (Q Wang) and ljmniat@126.com (J M Luo)

Received 28 September 2019, revised 3 December 2019
Accepted for publication 19 December 2019
Published 8 January 2020

Abstract

Interface adhesion and stability between titanium and carbon materials have been investigated by first-principles calculation, in which three different DFT-PBE, DFT-LDA and optB88-vdW approaches are considered. Our calculation reveals that the formation of carbon vacancy in graphene would enhance the interface stability and increase interfacial strength, which may be due to a strong hybridization between titanium atom and the sp^2 dangling bonds of the carbons near the vacancy. It is also found that the van der Waals interaction has less effects on cohesion properties of the titanium/graphite interfaces, and the Ti-C bond of titanium–carbon interfaces is weaker than that of the TiC bulk. The derived results are discussed in depth by means of electron distribution and Bader transfer analysis, and could be used as a guiding parameter for exploring the fundamental properties of titanium–carbon products as well as various potential applications.

Keywords: titanium–carbon interfaces, cohesion strength, stability, first-principles calculation, vdW interaction

(Some figures may appear in colour only in the online journal)

1. Introduction

In the past decades, titanium (Ti) has attracted enormous interests and has been potential applications in various areas such as aerospace, biomedicine, chemical plants, military, etc [1–4], mainly due to its high melting point, low density, high mechanical strength at room temperature, great corrosion behavior and biocompatibility [5–7]. Unfortunately, the pure titanium in the above application has been limited by some drawbacks such as poor high-temperature mechanical properties, low thermal conductivity and wear resistance [8–10].

To overcome the above disadvantages, one of the possible solutions is to add carbon materials in titanium, e.g. graphene, carbon nanotubes and carbon fibers, etc [11–13]. It is well accepted that the cohesion properties of Ti/graphene and Ti/graphite interfaces should play an important role in the performance of various Ti–C products. In this respect, there are already various experimental and theoretical studies in the literature [5, 7, 12–16]. However, to our best knowledge, there is not any study to compare the cohesion strength between Ti/graphene and Ti/graphite interfaces. In addition, the process of graphene synthesis should miss carbon atoms and form carbon vacancy defective graphene (CVG) [17, 18], which has been found to be the higher activity for adsorption of atoms and

[4] Author to whom any correspondence should be addressed.

nanoparticles than pristine graphene [19, 20]. Interestingly, the CVG could been formed by such experimental methods as treatment of hydrochloric acid [21] and electron beam irradiation [22]. Nevertheless, it should be noted that the stability of Ti/CVG interfaces is far from systematic investigation in the literature.

By means of highly accurate first principles calculation based on density functional theory, the pursuing aim is to find out the cohesion properties and stability of Ti–C interfaces. In the present study, the interface strength and interface energies of Ti/graphene, Ti/CVG, and Ti/graphite have been gained for comparison, and the mechanism would be revealed in terms of electron distribution and Bader transfer analysis. It will be shown that the derived results are not only in good agreement with similar experimental observations in the literature, but also provide a detailed understanding of interface cohesion of Ti–C system.

2. Theoretical methods

We performed calculations and optimized geometries with the Vienna *ab initio* simulation package (VASP) code [23, 24]. The present computation uses the projector augmented wave (PAW) potentials [25], which expresses electronic exchange-correlations by the generalized gradient approximation (GGA) of Perdew–Burke–Ernzerhof (PBE) [26] and local density approximation (LDA) [27]. The Kohn–Sham wave functions are expanded in a plane-wave basis set with an energy cutoff of 500 eV. The methods of Methfessel-Paxton [28] and Blöchl–Jepsen–Andersen [29] are employed for the dynamical and static calculations, respectively.

The systematic calculation of Ti–C interfaces would be a challenging work due to the van der Waals force of C–C and C–Ti layers, which has important effects on interface cohesion. To deal with this issue, several density functional theories have been thus proposed in the literature [30, 31]. For instance, the SAPT(DFT) method produced accurate results on the TiO_2 surface [32], and the vdW-DF method also accurately predicted experimental results [33, 34]. In this work, we mainly considered vdW-DF method, which is a non-local correlation functional that approximately accounts for dispersion interactions [31]. The original revPBE exchange has been replaced by the optB88 exchange functional developing by Klimeš and Michaelides [35, 36].

It is difficult to match between Ti and C since a big lattice mismatch. To obtain a small lattice mismatch, a 2×2 surface unit cell of Ti (0001) and graphite (0001) planes is chosen in the present investigation. For each interface structure, the lattice size of graphene and graphite is the optimized value 2.45 Å, and a certain number (1–5) of Ti-layers plus 20 Å vacuum distance are strained to fit onto the surface unit cell of graphene and graphite. Note that five carbon layers are selected for the Ti/graphite interface, and the lattice mismatch of Ti is only 1.8% compared with the optimized value 2.880 Å. As a typical example, figure 1 demonstrates the Ti/graphite, Ti/graphene, Ti/CVG interfaces with five Ti-layers. It can be seen clearly from this figure that the Ti/CVG interface is structured by missing a carbon atom from Ti/graphene interface.

The relaxation and static calculations are conducted in k-meshes of $9 \times 9 \times 1$ and $11 \times 11 \times 1$, respectively, together with a k-point broadening of $13 \times 13 \times 1$ for the electron distribution and Bader analysis. In order to improve the computation efficiency during the optimization, the bottom Ti-layer is fixed as the reference of the relaxation of other interface atoms. The force criterion acting on each atom during relaxation is 1.0×10^{-3} eV Å^{-1}, and the total energy converged 1.0×10^{-3} meV/atom.

3. Results and discussion

Prior to selecting suitable theoretical method, the lattice constant as well as cohesive energy and bulk modulus of graphite and α-titanium are calculated by means of DFT-PBE, DFT-LDA and optB88-vdW approaches, and the derived results are listed in table 1. To have a comparison, the corresponding experimental values are also presented in this table [37–42]. It can be seen clearly from this table that ground-state properties of graphite derived from DFT-LDA and optB88-vdW are closer to the experimental values in the literatures [38, 40, 41], however, the data of α-titanium calculated from the optB88-vdW and DFT-PBE matches well with the similar experimental results [37–39]. It should be pointed out that the *c*/*a* value and bulk modulus of graphite have not been predicted accurately in terms of DFT-PBE approach. Our further research reveals that the negative interfacial strength appears in several Ti–C interfaces by DFT-PBE and DFT-LDA methods. Such an unphysical phenomenon has been inconsistent with the chemisorption interface of Ti/graphene from experiments [42, 43]. Thus, DFT-PBE and DFT-LDA are not the best for simulating system with strong vdW interactions, and the optB88-vdW method is adopted in the following interface calculations.

We first consider the interface work of separation (W_{sep}), and the results of Ti–C interfaces are obtained from the following expression:

$$W_{sep} = \frac{E_{Ti\text{-layer}} + E_{C\text{-layer}} - E_{Ti/C}}{A}, \quad (1)$$

here $E_{Ti/C}$ and A are total energy and surface area of the Ti–C interface, $E_{Ti\text{-layer}}$ and $E_{C\text{-layer}}$ represent the total energy of the isolated Ti and graphite/graphene slabs, respectively. Generally speaking, the interfacial strength can be described directly by means of the derived work of separation, i.e. the higher work of separation normally means more stronger interfacial strength, and vice versa.

After a series of calculations, figure 2(a) demonstrates the work of separation of Ti–C interfaces as a function of the number of Ti-layer. It can be observed clearly that the W_{sep} values of Ti/graphene, Ti/CVG, and Ti/graphite interfaces show a convergence trend when the number of Ti-layer reaches four. A detailed analysis would find that the W_{sep} of Ti/graphene interface with four and five Ti-layers is 2.10 and 2.11 J m^{-2}, respectively, which is amazing consistency with the value of 2.12 J m^{-2} from molecular dynamics simulation using the COMB3 potential [14]. Such a big positive value indicates that the Ti/graphene interface has formed chemical

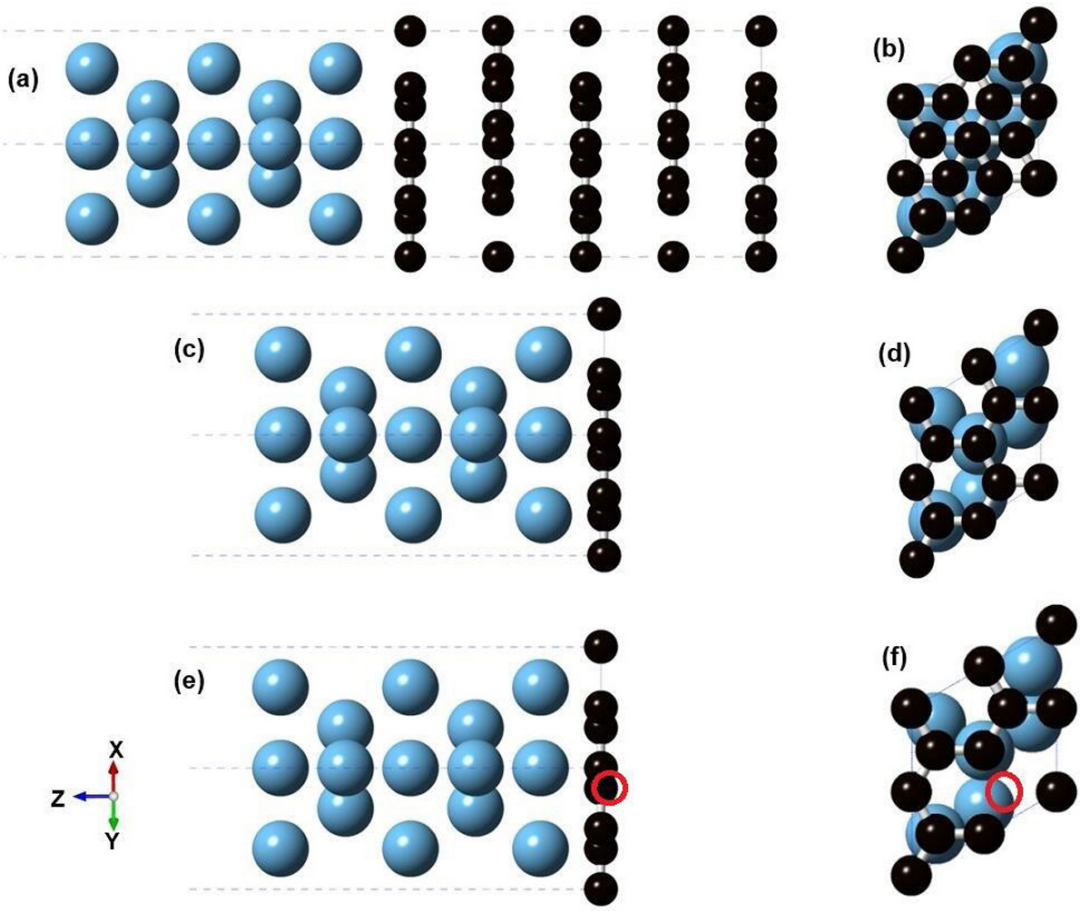

Figure 1. Schematic illustrations of various Ti/C interfaces. The (a) side and (b) top views of Y-X projection of prefect Ti(0 0 0 1)/graphite(0 0 0 1) interface, the (c) side and (d) top views of Y-X projection of prefect Ti(0 0 0 1)/graphene interface, and the (e) side and (f) top views of Y-X projection of Ti(0 0 0 1)/CVG interface. The big blue and small black balls represent Ti and C atoms, respectively.

Table 1. Comparison of lattice constants, cohesive energy, and bulk modulus of graphite and α-titanium from the different theoretical methods. The corresponding experimental data in the literature are also listed.

	Parameter	DFT-PBE	DFT-LDA	optB88-vdW	Exp.
Graphite	a (Å)	2.47	2.45	2.45	2.46[a]
	c/a	3.51	2.72	2.68	2.72[a]
	E_0 (eV)	8.2	8.9	8.3	7.4[b]
	B (GPa)	2.85	21.87	32.44	33.8[c]
Titanium	a (Å)	2.924	2.858	2.880	2.940[d]
	c/a	1.581	1.575	1.574	1.591[d]
	E_0 (eV)	5.35	6.14	5.59	4.85[b]
	B (GPa)	116.5	131.8	121.8	110.1[e]

[a] Lipson and Stokes[37].
[b] Kittel [38].
[c] Hanfland *et al* [39].
[d] San-Martin and Manchester [40].
[e] Fisher and Renken [41].

interaction, which is in good agreement with the experimental evidences [42, 43].

Interestingly, we can also discern form figure 2(a) that the W_{sep} of Ti/graphite interface is 2.08 J m^{-2}, which is very close to the value of Ti/graphene interface. This result suggests that the increasing of the underlying graphite layer almost has a negligible influence on interface cohesion. The main reason would be probably due to the van der Waals interaction of graphite layers, which is much weaker than Ti–C chemical bonds of the interface. In addition, the descending sequence of W_{sep} values of Ti/graphene, Ti/CVG, and Ti/graphite interfaces with four and five Ti-layers are as follows: Ti/CVG → Ti/graphene → Ti/graphite, and the W_{sep} of Ti/CVG interface (5.15 J m^{-2}) are more than twice bigger than that of Ti/graphene

and Ti/graphite interfaces. In other words, the introduction of single carbon vacancy defect in graphene greatly enhance the interfacial strength of Ti–C interfaces. The fundamental mechanism of interface cohesion will be revealed in the following paragraphs.

To further investigate interface stability, the interface energy (E_{int}) is then computed as follows [44]:

$$E_{\text{int}} = \frac{E_{\text{Ti/C}} - \text{E}_{\text{bulk-Ti}} - E_{\text{bulk-C}}}{A} - \sigma_{\text{Ti}} - \sigma_{\text{C}}, \qquad (2)$$

where $E_{\text{Ti/C}}$ and A have the same meanings as before of the equation (1), $E_{\text{bulk-Ti}}$ and $E_{\text{bulk-C}}$ are bulk energies of the α-Ti and graphene/graphite layers, respectively. σ_{Ti} and σ_{C} are surface energies of Ti and graphite/graphene slabs, respectively, which are derived from the following expression:

$$\sigma = \frac{1}{2}(E_{\text{tot}}^{\text{slab}} - E_{\text{tot}}^{\text{bulk}}), \qquad (3)$$

here $E_{\text{tot}}^{\text{slab}}$ is the total energy of the slab, and $E_{\text{tot}}^{\text{bulk}}$ is the total energy of the corresponding bulk.

The E_{int} values of Ti/graphene, Ti/CVG, and Ti/graphite interfaces are computed as a function of the number of Ti-layer, and the derived results are shown in figure 2(b). Several features could be deduced from this figure. Firstly, the E_{int} values of all the Ti–C interfaces also converge reasonably well as mentioned above, while with the increasing number of Ti-layer, the E_{int} trends of three interfaces seem opposite of the W_{sep} curves shown in figure 2(a). Such a coincidence indicates that the interface energy has a direct correlation with the work of separation, i.e. a higher interfacial strength probably means a more lower interface stability, and vice versa.

Secondly, it clearly shows that the E_{int} values of Ti/CVG interface are much smaller than that of Ti/graphene and Ti/graphite interfaces, predicting that the Ti/CVG interface would be thermodynamically more stable. That is to say, the interfaces between titanium and carbon should be formed preferentially around carbon vacancies, which matches well with the experimental observation in the literature [45]. Thirdly, the E_{int} value of Ti/CVG interface with four and five Ti layers are -1.64 and -1.71 J m^{-2}, respectively. Such small and negative values indicate a strong hybridization between Ti atoms and defective graphene.

It is of importance to identify the root cause why the Ti/CVG interface has stronger interfacial strength than the Ti/graphene and Ti/graphite interfaces. Accordingly, the charge density difference of the all interfaces are calculated. As a typical example, figure 3 illustrates the charge density difference of the relaxed Ti–C interfaces with four Ti-layers, which is obtained by subtracting charge density of isolated Ti and graphene/graphite slabs. It should be noted that the yellow and slight blue regions correspond the charge accumulation and depletion, respectively. In addition, in order to have a clear expression in the following paragraphs, the A, B and C shown in figure 3 are used to represent the first carbon, the first titanium and second titanium layers, respectively.

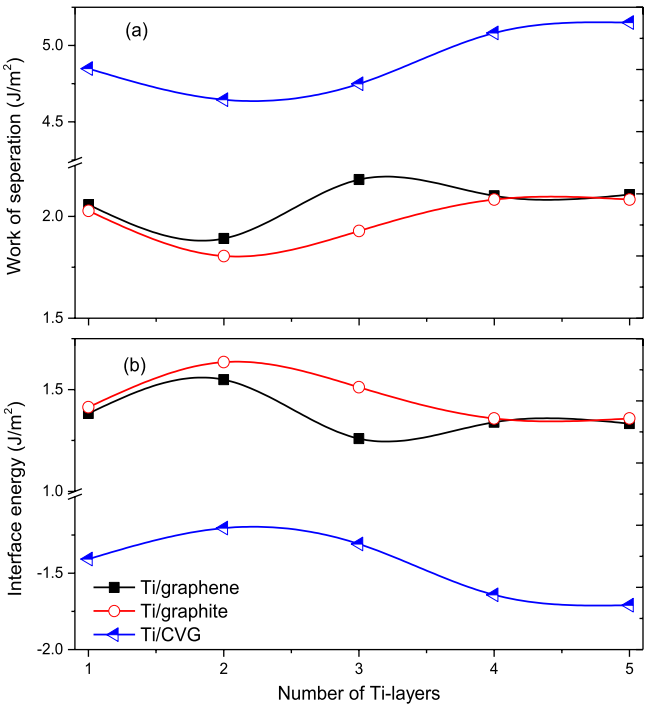

Figure 2. (a) Work of separation (W_{sep}) and (b) interface energy (E_{int}) of Ti/graphene, Ti/graphite and Ti/CVG interfaces.

One can discern from figure 3 that the charge transfer of the Ti/graphite interface is localized in A layer and will not affect the underlying graphite layer. The result gives a visualized picture for interpreting the negligible effects of van der Waals interaction, which is reflected by the comparison of W_{sep} and E_{int} of Ti/graphene and Ti/graphite interfaces as before. Moreover, the charge transfer from the interfacial Ti to C in all interfaces are directional and dense, suggesting that chemical bonds have been formed between interfacial Ti and C atoms, which brings about a deep understanding to the strong interfacial strength. In addition, the charge transfer of the prefect Ti/graphene and Ti/graphite interfaces mainly locates between A and C layers, while limiting between A and B layers in the Ti/CVG interface. The charge density difference analysis reveals that charge transfer between Ti and defective graphene is significantly increased, suggesting the formation of a stronger Ti–C bonding.

To systematically compare the bond charge of Ti-C interfaces, the Bader charger analysis is selected and applied between Ti and C atoms in the Ti/graphene, Ti/CVG, and Ti/graphite interfaces with four Ti layers. Table 2 lists the average bond charge of Ti-C in A and B layers, and the corresponding data of B1-TiC bulk are also calculated for the sake of comparison. As illustrated in this table, the average bond charge of Ti atom is -0.607 e in the Ti/CVG interface, which is around 0.3 e larger than that of the Ti/graphene and Ti/graphite interfaces. The same phenomenon of average bond charge can also be found in C atoms. The transferred charge further confirms that the chemical bonds maked in the Ti/CVG interface have be much stronger than that in Ti/graphene and Ti/graphite

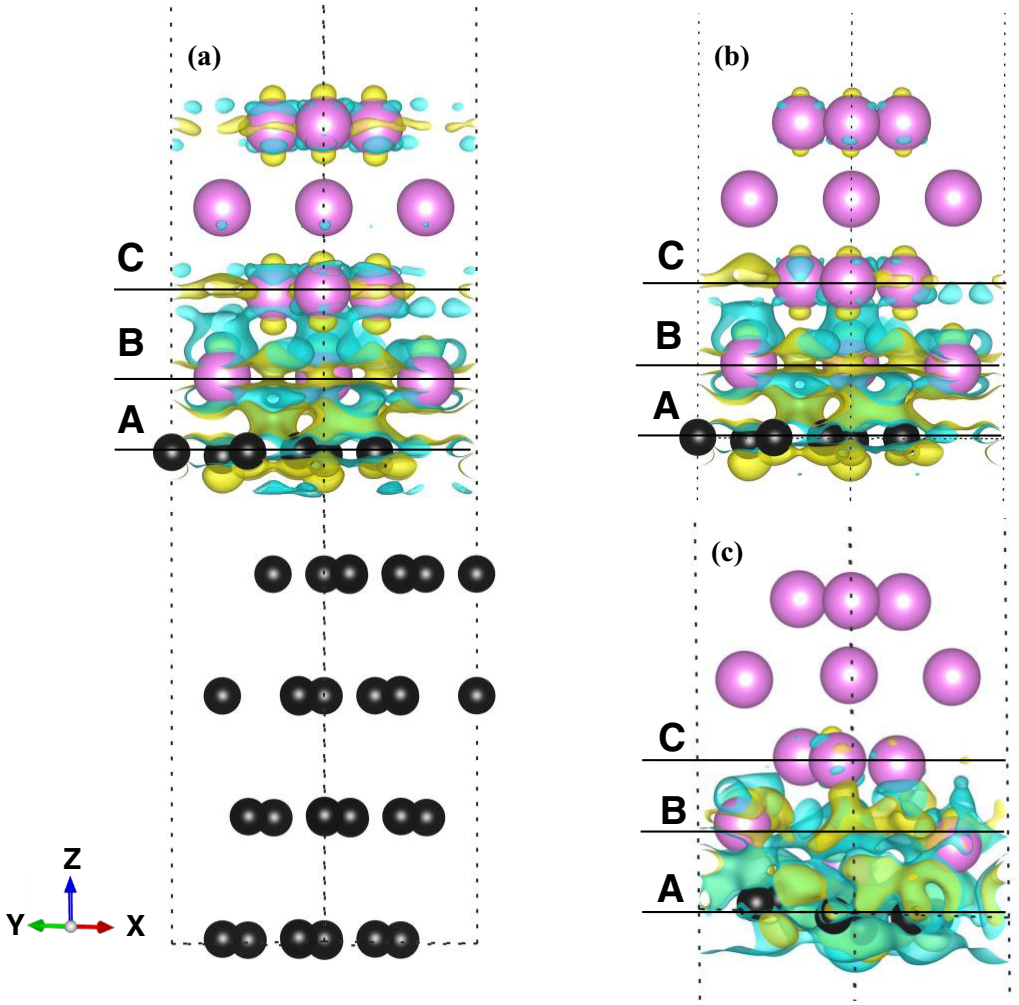

Figure 3. Charge density difference of the relaxed Ti–C interfaces with four Ti-layers. (a) Ti/graphite interface, (b) Ti/graphene interface, and (c) Ti/CVG interface. The big blue and small black balls represent Ti and C atoms, and the isosurface value is set to 0.001 e/Bohr^3.

Table 2. Average bond charge of Ti-C in A and B layers of Ti/graphene, Ti/graphite and Ti/CVG interfaces shown in figure 3. The corresponding data of B1-TiC bulk are also calculated and listed for comparison, and the symbol of '+' and '–' represents the charge gain and charge loss, respectively.

		Average bond charge (e/atom)	
Type		C	Ti
Interface	Ti/graphene	+0.149	−0.358
	Ti/graphite	+0.140	−0.355
	Ti/CVG	+0.253	−0.607
Carbides	TiC	+1.394	−1.394

interfaces. There is a need of further research into the fundamental reason that average bond charge of the Ti/CVG interface increased dramatically. At the same time, we find that the one Ti atom neighboring the vacancy has much bigger bond charge (−1.09 e) than the others (−0.46 and −0.27 e), which may be the primary cause why the average bond charge of the Ti/CVG interface increases multiply. Such a big value of transferred charge should be due to a strong hybridization between Ti atom and the sp^2 dangling bonds of the carbons near the vacancy. Additionally, the charge transfers between Ti and C atoms in Ti-C interfaces are much smaller than those in the bulk of titanium carbides, which predicts that the Ti–C bonds formed in the interface have be weaker than those in the bulk.

Consequently, figure 4, as another example, plots the comparison of total density of states (TDOS) of the Ti/graphene and Ti/CVG interfaces with four Ti-layers. As expected, the TDOS of the Ti/CVG interface has a smaller bandwidth, and its peaks located at about −0.5 and −3.75 eV below the Fermi level (E_F) are bigger than that of the Ti/graphene interface. The above comparison of electronic structures suggests that the interaction between Ti and defective graphene should be stronger than the pristine Ti/graphene interface, which would intrinsically bring about the excellent cohesion properties of the Ti/CVG interface shown in figure 2.

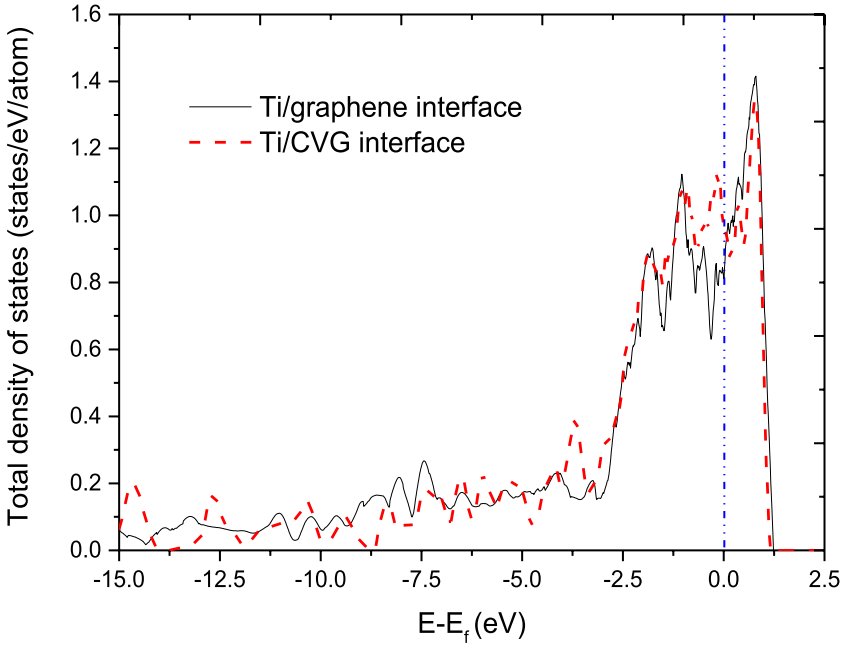

Figure 4. Total density of states (TDOS) of the Ti/graphene and Ti/CVG interfaces with four Ti-layers.

4. Conclusions

In summary, we have carried out the systematic investigation of the work of separation and interface energy of the Ti/graphene, Ti/CVG, and Ti/graphite interfaces using first-principle calculation. To deal with the van der Waals force in present system, the optB88-vdW method is selected after a series of tests. The results show that the Ti/CVG interface has a bigger work of separation and lower interface energy than the Ti/graphene and Ti/graphite interfaces, suggesting that the interaction between Ti and defective graphene should be much stronger than pristine Ti/graphene interfaces. Our results also reveal that the work of separation and interface energy of the Ti/graphene are very close to the corresponding values of the Ti/graphite interface, suggesting the van der Waals forces of graphite layers are much weaker than Ti-C chemical bonds of the interface. The simulations not only match well with experimental evidences in the literature, but also give a deeper understanding of interface cohesion in terms of charge density difference and Bader transfer analysis.

Acknowledgment

This research work was supported by Foundation of Nanchang Hangkong University (Grant No. EA201901093), Natural Science Foundation of Jiangxi Province (Grant No. 20171BAB216002), and National Natural Science Foundation of China (Grant No. 51764041 and 51463017).

ORCID iDs

Liang Chen https://orcid.org/0000-0003-2419-480X
Qian Wang https://orcid.org/0000-0001-5540-3649

References

[1] Lütjering G and Williams J C 2007 *Titanium* (Springer: Heidelberg)
[2] Liu X, Chu P K and Ding C 2004 *Mater. Sci. Eng.* R **47** 49
[3] McDonnell S, Smyth C, Hinkle C L and Wallace R M 2016 *ACS Appl. Mater. Interfaces* **8** 8289
[4] Dehghan-Manshadi A, Bermingham M J, Dargusch M S, StJohn D H and Qian M 2017 *Powder Technol.* **319** 289
[5] Mu X N, Cai H N, Zhang H M, Fan Q B, Zhang Z H, Wu Y, Ge Y X and Wang D D 2018 *Mater. Des.* **140** 431
[6] Niinomi M 1998 *Mater. Sci. Eng.* A **243** 231
[7] Yang W Z, Huang W M, Wang Z F, Shang F J, Huang W and Zhang B Y 2016 *Acta Metall. Sin.* **29** 707
[8] Nemat-Nasser S, Guo W G and Cheng J Y 1999 *Acta Mater.* **47** 3705
[9] Ezugwu E O and Wang Z M 1997 *J. Mater. Process. Technol.* **68** 262
[10] Attar H, Prashanth K G, Chaubey A K, Calin M, Zhang L C, Scudino S and Eckert J 2015 *Mater. Lett.* **142** 38
[11] Nieto A, Bisht A, Lahiri D, Zhang C and Agarwal A 2017 *Inter. Mater. Rev.* **62** 241
[12] Montealegre Melendez I, Neubauer E, Angerer P, Danninger H and Torralba J M 2011 *Compos. Sci. Technol.* **71** 1154
[13] Li F X, Hao P D, Yi J H, Chen Z, Prashanth K G, Maity T and Eckertb J 2018 *Mater. Sci. Eng.* A **722** 122
[14] Fonseca A F, Liang T, Zhang D, Choudhary K, Phillpot S R and Sinnott S B 2017 *ACS Appl. Mater. Interfaces* **9** 33288
[15] Gong C, Lee G, Shan B, Vogel E M, Wallace R M and Cho K 2010 *J. Appl. Phys.* **108** 123711
[16] Khomyakov P A, Giovannetti G, Rusu P C, Brocks G, van den Brink J and Kelly P J 2009 *Phys. Rev.* B **79** 195425
[17] Geng D S, Chen Y, Chen Y G, Li Y L, Li R Y, Sun X L, Ye S Y and Knights S 2011 *Energy Environ. Sci.* **4** 760
[18] Lahiri J, Lin Y, Bozkurt P, Oleynik I I and Batzill M 2010 *Nat. Nanotechnol.* **5** 326
[19] Lee G D, Wang C, Yoon E, Hwang N M, Kim D Y and Ho K 2005 *Phys. Rev. Lett.* **95** 205501

[20] Lim H D, Negreira A S and Wilcox J 2011 *J. Phys. Chem.* C **115** 8961
[21] Coleman V, Knut R, Karis O, Grennberg H, Jansson U, Quinlan R, Holloway B, Sanyal B and Eriksson O 2008 *J. Phys. D: Appl. Phys.* **41** 062001
[22] Hashimoto A, Suenaga K, Gloter A, Urita K and Iijima S 2004 *Nature* **430** 870
[23] Wang Q, Du G P, Chen N and Jiang C S 2019 *Int. J. Hydrogen Energy* **44** 26469
[24] Chen L, Wang Q, Xiong L and Gong H R 2018 *J. Alloys Compd.* **747** 972
[25] Kresse G and Joubert J 1999 *Phys. Rev.* B **59** 1758
[26] Perdew J P, Burke K and Ernzerhof M 1996 *Phys. Rev. Lett.* **77** 3865
[27] Perdew J P and Zunger A 1981 *Phys. Rev.* B **23** 5048
[28] Methfessel M and Paxton A T 1989 *Phys. Rev.* B **40** 3616
[29] Blöchl P E, Jepsen O and Andersen O K 1994 *Phys. Rev.* B **49** 16223
[30] Grimme S 2011 *WIREs Comput. Mol. Sci.* **1** 211
[31] Dion M, Rydberg H, Schröder E, Langreth D C and Lundqvist B I 2004 *Phys. Rev. Lett.* **92** 246401
[32] Tamijani A A, Salam A and de Lara-Castells M P 2016 *J. Phys. Chem.* C **120** 18126
[33] Zhang W B, Chen C and Tang P Y 2014 *J. Chem. Phys.* **141** 044708
[34] Liu W, Filimonov S N, Carrasco J and Tkatchenko A 2013 *Nat. Commun.* **4** 2569
[35] Klimeš J, Bowler D R and Michaelides A 2011 *Phys. Rev.* B **83** 195131
[36] Klimeš J, Bowler D R and Michaelides A 2010 *J. Phys.: Condens. Matter.* **22** 022201
[37] Lipson H and Stokes A R 1942 *Nature* **149** 328
[38] Kittel C 1996 *Introduction to Solid State Physics* (New York: Wiley)
[39] Hanfland M, Beister H and Syassen K 1989 *Phys. Rev.* B **39** 12598
[40] San-Martin A and Manchester F D 1987 *Bull. Alloy Phase Diagr.* **8** 30
[41] Fisher E S and Renken C J 1964 *Phys. Rev.* **135** A482
[42] Pirkle A, Wallace R M and Colombo L 2009 *Appl. Phys. Lett.* **95** 133106
[43] Hsu A L *et al* 2014 *ACS Nano* **8** 7704
[44] Lee S J, Lee Y K and Soon A 2012 *Appl. Surf. Sci.* **258** 9977
[45] Mashoff T, Convertino D, Miseikis V, Coletti C, Piazza V, Tozzini V, Beltram F and Heun S 2015 *Appl. Phys. Lett.* **106** 083901